 doi:10.20944/preprints201812.0141.v1

Investigation of Corrosion Resistance of poly(o-phenylenediamine)-ZnO Composites on Carbon Steel

Chaogang Zhou [1], Chaojin Zhou [2], Jiawei Zhang [3,*]

1 College of Metallurgy and Energy, Key Laboratory of the Ministry of Education for Modern Metallurgy Technology, North China University of Science and Technology, Tangshan 063009, China；zhouchaogang9@163.com

2. School of Materials Science and Engineering, Guangdong Provincial Key Laboratory of Advanced Energy Storage Materials, South China University of Technology, Guangzhou 510641, China；mszcj@mail.scut.edu.cn

3. School of Metallurgy, Northeastern University, Shenyang 110819, China

* Corresponding author：1600811@stu.neu.edu.cn

Abstract: Synthesis of poly(o-phenylenediamine) (PoPD) and poly(o-phenylenediamine)-ZnO (PoPD-ZnO) nanocomposites on carbon steel by in-situ polymerization with HCl acid as doping acid Material coating. The composition and structure of PoPD-ZnO nanocomposites were characterized by Fourier transform infrared spectroscopy (FTIR), X-ray diffraction (XRD) and scanning electron microscopy (SEM). The corrosion protection ability of polymer coatings in 3.5% NaCl was studied by potentiodynamic polarization curves and electrochemical impedance spectroscopy. It can be seen from the electrochemical corrosion experimental data that PoPD-WPU coating (PWC) and PoPD-ZnO-WPU coating (PZWC) can effectively improve the corrosion resistance of the carbon steel substrate, and the corrosion rate is reduced by 2-3 orders of magnitude compared with carbon steel. The conclusion demontrates that PoPD can effectively extend the service life of carbon steel substrates. In addition, it is advantageous to form a compact and low-defect coating when added nano-particle ZnO, which is advantageous for the POPD film to develop its good barrier property and corrosion resistance.

Keywords: poly(o-phenylenediamine) (PoPD); ZnO; WPU; polymer coating; anticorrosion

1. Introduction

Conductive polymers (CPs) have been studied for the replacement of electronic devices, optoelectronics, and semiconductor materials due to their mechanical strength, electrical conductivity, corrosion stability and possibility of both chemical and electrochemical synthesis [1-3]. The benzene ring and the π bond are usually present in the polymer, which facilitates electron transport of the polymer and the external environment, thereby making them useful in wide area of applications. The charge is located on the area of several repeating units such as benzene ring and the π bond, which is considered as a charge carrier in conductive polymers. The repeating units facilitate local charges move along the polymer chain, and thereby make them useful in the wide area of applications [4]. At this background, (poly-aniline) (PANI) and its derivatives (such as polypyrrole and polythiophene) attract much research interest due to advantages like easy synthesizability, better doping ability, architecture flexibility, environmental stability, wide applicability, etc [5].

An important role in corrosion resistance is played by conductive polymers-inorganic oxide nanocomposites [6]. In the field of corrosion, a number of studies have been carried out to design CPs-inorganic filler composite coatings with good corrosion resistance, such as SiO_2, TiO_2, ZnO, carbon nanotubes and graphene oxide (GO) [7-11]. Inorganic fillers, nano-ZnO particles have

Preprints (www.preprints.org) | NOT PEER-REVIEWED | Posted: 12 December 2018 doi:10.20944/preprints201812.0141.v1

attracted extensive attention due to their environmentally friendly properties [12,13], low cost, excellent mechanical and chemical stability. Most polymers are insulators due to their electron mobility limitations. The conductive polymer is a semiconductor material that can be doped and converted into a conductive polymer. Doping acid into the polymer can form a hole conductor (p-type) material, and ZnO is a good electron acceptor (n-type), when they are mixed together, they form a p-n structure and greatly increase the electron transfer ability [14].

Although PANI exhibits good corrosion resistance, the poor processability of PANI powder and the low adhesion to metal substrates severely limit its application. PODP is a derivative of PANI, and its introduction of electron donating group significantly improve the physical properties and corrosion resistance of PANI [15]. PoPD is very stable in acid, neutral, and alkaline solutions and air and can prepare in above aqueous [16]. It has apparently different molecular structure when compared with PANI. Unlike the parent polymer polyaniline which has a linear structure, PoPD is a ladder-type polymer [17]. It has been reported that there existence a highly aromatic hydrocarbon polymer containing repeating units of 2,3-diaminophenazine or quinoxaline [18,19]. Additionally, the electrochemical and physical properties of PoPD differ significantly from polyaniline. When the potential is increased to +1 V, PoPD is less prone to electrochemical degradation, while polyaniline is not. Compared with PANI, PoPD has extremely high thermal stability and strong adsorption [18-21].

Luis et al. has been electrosynthesized PoPD films on 304 stainless steel in aqueous solution of phosphoric acid. They noted that the reduced form of PoPD in a translucent green state provides a fairly good protection against pitting for steel in highly aggressive chloride medium [22]. Aboozar et al. found that the nanocomposite coating compared with pure polyester coating provided a coating with a lower number of pores and provide a better corrosion resistance. In addition to providing a barrier against diffusion of electrolyte, ZnO nanoparticles act as a corrosion inhibitor and thus increases the corrosion resistance [23].

To the best of our knowledge, few literature on the coating of PoPD-ZnO nanocomposites has been published as corrosion protection for carbon steel in chloride media [24]. In this paper, we used carbon steel as the substrate, and prepare nanocomposite coatings composed of PoPD and PoPD-ZnO by chemical oxidation. The structure and properties of PoPD-ZnO nanocomposites were studied. The corrosion resistance of PoPD-ZnO nanocomposite coatings on carbon steel samples was studied at room temperature with 3.5% NaCl.

2. Experimental

2.1 Materials

O-Phenylenediamine monomers were obtained from Beijing Infinity Scientific Co., Ltd. Ammonium persulfate ($(NH4)_2S_2O_8$, APS) and nanoparticles ZnO (99.9 %, 30 ± 10 nm) were purchased from Shanghai Aladdin Biochemical Technology Co., Ltd. Butyl alcohol, dibutyl phthalate, ethyl acetate and sodium chloride (NaCl) were purchased from Tianjin Fuchen Chemical Reagent Co., Ltd. Hydrochloric acid (HCl) was purchased from Jinan Kunfeng Chemical Co., Ltd. N-methyl-2-pyrrolidone (NMP) was purchased from Damao Chemical Reagent Co., Ltd. Waterborne polyurethane (WPU) purchased from Jiaxing Dongjing Printing and Dyeing Material Co., Ltd.

2.2 Synthesis of steel coupons

The carbon steel of dimension 2cm × 2cm were mechanically polished with a series of emery papers (grade 320, 600, 1000), and this was followed by washing and degreasing with acetone and double distilled water and lastly dried in air.

2.3 Synthesis of poly(o-Phenylenediamine)-ZnO composite powders

Preprints (www.preprints.org) | NOT PEER-REVIEWED | Posted: 12 December 2018 doi:10.20944/preprints201812.0141.v1

poly(o-Phenylenediamine) (PoPD) and poly(o-Phenylenediamine)-ZnO (PoPD-ZnO) were synthesized by in situ emulsion polymerization method, and a given amount of HCl and monomers were mixed according to the molar ratio of 1:1. The typical chemical oxidative polymerization process of PoPD is as follow: 5.4 g of o-Phenylenediamine was added into 50 ml of 1 M HCl under a series of ultrasonic vibrating, magnetic and vigorous stirrings, and then 50 mL of 1 M APS solution was added dropwise into the above solution. The resulting mixture was allowed to react for 20hrs below 5 °C. After that, the precipitate was filtered and washed using double distilled water and ethanol to remove extra acid and oxidant until the filtrate into colorless, and then moved them in the vacuum oven to dry at 60 °C for 24hrs. PoPD-ZnO nanocomposite was synthesized by dispersing 0.25g of ZnO nanoparticles to the mixture of o-Phenylenediamine and HCl (The content is the same as the above process). The synthesis of the nanocomposite was further preceded following the identical procedure as prescribed for the synthesis of the copolymer [25].

2.4 Preparation of poly(o-Phenylenediamine)-ZnO/WPU composite coatings

The composite coating was fabricated by solution casting method. For the preparation of coating, 0.2 g of as-prepared PoPD-ZnO was suspended in 0.4 ml NMP and 0.2ml ethyl acetate. 1g WPU and 0.2g Hexamethylene Diisocyanate (HDI) were dispersed in the above solution by ultrasound. Pre-treated steel coupons were coated by using a solution casting method. The thickness of all coating films were measured by AIRAJ micrometer, which was about 480 ± 3 μm. Then cured to achieve a constant weight for each steel sample (approximately 60 °C for 12 hrs drying is needed) and PoPD-ZnO-WPU coating is abbreviated as PZWC. The preparation of the PoPD-WPU coatings (the content of PoPD is 0.2 g and abbreviated as PWC) was following the identical procedure as prescribed for the preparation of the PoPD-ZnO coatings. Figure 1 shows the schematic diagram preparation of poly(o-phenylenediamine)-ZnO coatings onto the carbon steel substrate.

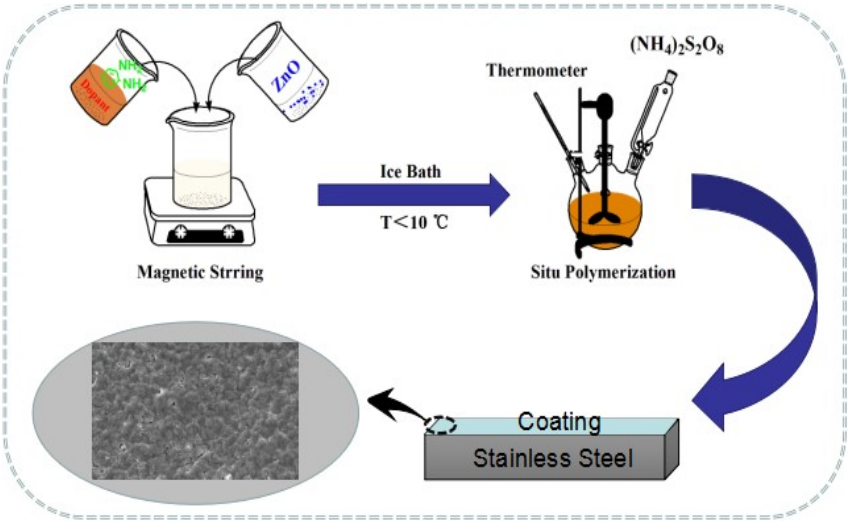

Figure 1. The schematic diagram preparation of poly(o-phenylenediamine)-ZnO coatings.

2.5 Characterization

The chemical structures of the samples were characterized on Fourier transform infrared spectroscopy (FTIR, Nicolet 6700) measurement in the range of 4000~500 cm^{-1} and X-ray diffraction (XRD) of the samples which were recorded in a Smart Lab X-ray diffractometer at 45kV/200mA, operating in the range of 10~90° (λ=0.15406 nm) with Cu K-alpha radiation. Morphology of the products and coatings were investigated by field emission scanning electron

Preprints (www.preprints.org) | NOT PEER-REVIEWED | Posted: 12 December 2018 doi:10.20944/preprints201812.0141.v1

microscopy (FESEM, EVO 18) with an acceleration voltage of 5 kV. Polarization curves and electrochemical impedance spectroscopy (EIS) measurements were carried out with CHI660E electrochemical workstation at room temperature. Polarization curves were measured by changing the potential from –1.2 to -0.2 V (vs. SCE) versus with a constant scan rate of 0.005 V/s, and the EIS curves were performed by utilizing a sine wave with 0.005 V amplitude under the frequency range of 10^5 Hz to 10^{-2} Hz, and the EIS data were analyzed by Zview software

3. Results and discussion

3.1 Structures and morphology of poly(o-Phenylenediamine)-ZnO

The FTIR spectra and XRD patterns of PoPD and PoPD-ZnO are shown in Figure 2. The polymerized PoPd in the presence and absence of ZnO was scraped off and FTIR spectra of the polymer powderswere recorded in (Figuer 2a). As shown in (Figuer 2a), the peaks at 1632 and 1530 cm^{-1} are attributed to the C=C stretching vibrations of quiniod (Q) and benzenoid (B) rings respectively. The C-N stretching vibrations of quinoid and benzenoid rings are appearing at 1365 and 1247 cm^{-1} respectively [26]. The two peaks appeared at 3320 and 3153 cm^{-1} are ascribed to the stretching vibrations of –NH– and $–NH_2$ respectively [27,28]. The PoPD-ZnO nanocomposites FTIR peaks are slightly shifted to higher or lower wavenumber when compared to PoPD. This may be due to the overlapping of peak related to the stretching of O–H bonding between ZnO nanoparticles and the N–H bond in PoPd chains. The absorption peaks coming from ZnO were detected in PoPd-ZnO indicating that the ZnO nanoparticles had loaded in PoPd successfully [28].

The XRD patterns of PoPD and PoPD-ZnO are illustrated in (Figure 2b). The XRD patterns results show the sharp peak around at 2θ=10° to 30°. These sharp peaks are indicating the partial crystalline nature of PoPD. The broad peak centered at 2θ=26.4° reveal that the local crystallinity may be caused by the periodicity perpendicular to the polymer chain [26,28,29]. The partial crystallinity may also result from the long range ordering of polymer chains and the doping of HCl. furthermore, Samanta indicates that the nature of the synthesized PoPD having well-alligned morphology was confirmed by the crystalline peaks located at 2θ = 10.7°, 16.6°, 18.4° and 28.8° [30]. In the XRD curve of PoPD-ZnO, the crystallization peaks at 2θ = 31.8°, 34.4°, 36.3°, 47.5° and 56.6° correspond to composite ZnO particles where is fully matching with JCPDS card No. 36-1451.

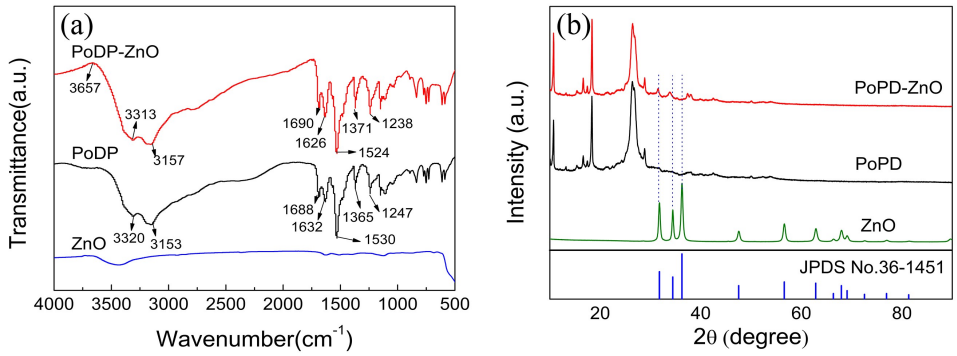

Figure 2. Structure analysis of PoPD and PoPD-ZnO: (a) FTIR spectra and (b) XRD patterns.

The surface morphologies of polymers were characterized by FESEM. As shown in Figure 3, the FESEM images of PoPD and PoPD-ZnO all show the aggregated structures. The PoPD exhibit a larger lumphy structure with the diameter range of 2-3 μm, and irregularly shaped sheets and granules attached to its surface. While PoPD-ZnO consists of a stack of stick-like structure that

Preprints (www.preprints.org) | NOT PEER-REVIEWED | Posted: 12 December 2018 doi:10.20944/preprints201812.0141.v1

with a size of about 1μm and smooth surface. From the FESEM images of PoPD-ZnO composites, it is confirmed that the morphology of PoPD is affected by ZnO nanoparticles. Combining the above two graphics of FTIR and XRD indicateing that ZnO nanoparticles are embedded in PoPD.

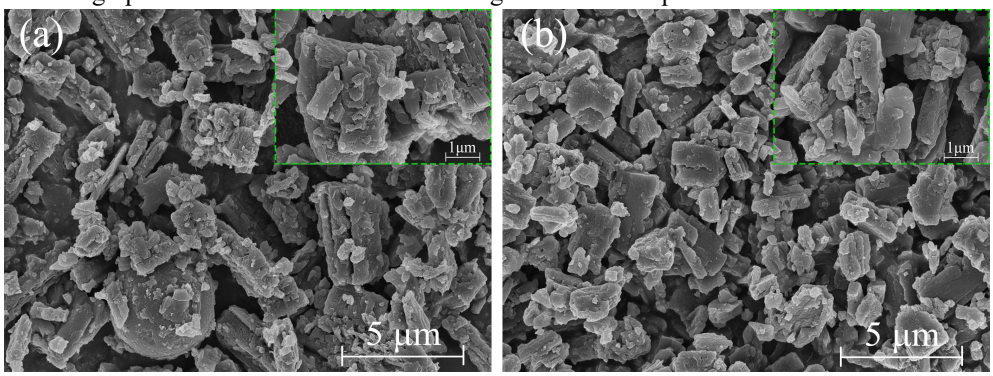

Figure 3. FESEM images of (a) PoPD and (b) PoPD-ZnO.

3.2 CV characterization of poly(o-Phenylenediamine)-ZnO Particles

The electrochemical activity and stability of POPD and POPD-ZnO were obtained by scanning the CV curves at a scan rate of 20 mVs^{-1} in 1.0 M HCl solution and are shown in Figure 4. In the acidic solution, H^+ exists in the acidic solution to facilitate the reversible redox reaction of the polymer, and the parameters obtained are more obvious than other solutions. As shown in (Figure 4a), the CV curves of POPD and POPD-ZnO are display distinct redox peaks, which indicates all materials have reversible electrochemical activity and pseudocapacitive charge storage properties. The reversibility of the electrochemical redox reaction can be estimated by the potential ratio between the oxidation peak and the reduction peak, and the closer to 1, the higher the reversibility. From (Figure 4a), we can estimate that the oxidation potential and the reduction potential of the potential POPD are about -0.097 and -0.17 V, respectively, and the oxidation potential and the reduction potential of the POPD-ZnO are about -0.1 and -0.15, respectively. The redox current value of POPD-ZnO is also about 2 times larger than POPD. This may be because the introduction of ZnO nanoparticles does not change the electrochemical reversibility of POPD, but it can exert a synergistic effect with POPD, promote the redox reaction of POPD chain, and make the electrochemical behavior of POPD-ZnO be better than POPD. As shown in (Figure 4b), with the number of scans increasing, the current response decreased and the corresponding redox peak shapes broadened, indicating the good electrochemical stability of all the obtained materials.

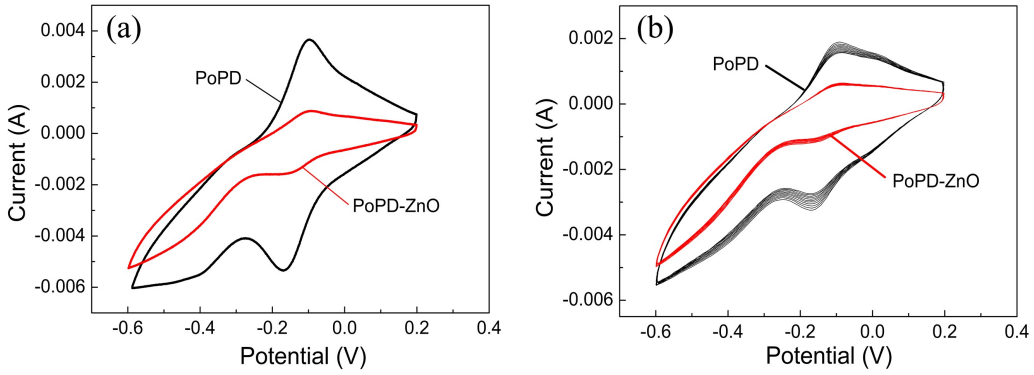

Figure 4. CVs of PoPD and PoPD-ZnO (a) 1 cyclic voltammograms, (b) 20 cyclic voltammograms.

Preprints (www.preprints.org) | NOT PEER-REVIEWED | Posted: 12 December 2018 doi:10.20944/preprints201812.0141.v1

3.3 Characterization of poly(o-Phenylenediamine)-ZnO coating surface morphology

Scanning electron microscopy (SEM) is extensively used in the surface analysis of synthesized materials. Figure 5 demonstrates the SEM micrographs of the WPU coating (Figure 5a), PWC (Figure 5b) and PWZC (Figure 5c). As can be seen, there are some defects structures on the surfaces of the PWC and PWZC. This is due to the fact that some of the oligomers become soluble in the acidic doping medium during doping. In addition, the presence of a doping medium affects the conductivity of the same type of polymer[26]. However, the porosity of the PoDP-ZnO is less than that of the PoDP, which is attributed to the fact that the polymer monomer can be effectively attached around the ZnO, increasing the degree of polymerization. On the other hand, ZnO can also be filled into the voids of the polymer, reducing the presence of voids.

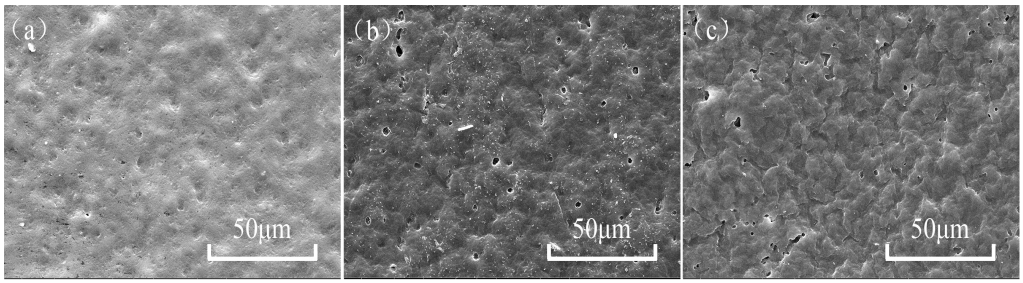

Figure 5. SEM images of (a) WPU coating, (b) PWC, (c) PWZC.

3.4 Corrosion protection evaluation of poly(o-Phenylenediamine)-ZnO Coating

The corrosion performances of PZWC and PWC coatings were measured after immersion in 3.5% NaCl solution for 168 h by potentiodynamic curves and EIS methods, as shown in (Figure 6). Polarization curves are illustrated in (Figure 6a), the corrosion characteristics of corrosion potential (E_{corr}) and corrosion current density (I_{corr}) calculated by the Tafel curves extrapolation method are listed in Table 1. The corrosion rate (CR) of the pristine and coated steels in Table 1 was calculated by the following equation [31].

$$CR = 3270 \times \frac{M(g) \cdot I_{corr}(A/cm^2)}{n \cdot \rho(g/cm^3)} \quad (1)$$

Where M is the molecular mass, it represents the molar mass of the working electrode metal. I_{corr} is corrosion current density, n is the number of electrons transferred by 1 mol of metal during the oxidation reaction, and ρ is the density of steel. As shown in (Figure 6a) and Table 1, also gives the corrosion parameters of WPU, PWC and PZWC coatings calculated by euation (1). A negative shift in CR values of 3 and 6-fold have been found when POPD and POPD-ZnO were applied to the WPU, respectively. The E_{corr} values of the samples protected with WPU and polymer coatings shifted positively relative to that of uncoated steel, indicating that all the coatings prevent corrosion to some extent. PZWC coating has a higher E_{corr} and lower I_{corr}, which indicates that it has good corrosion resistance compared to WPU, and PWC. This suggests that the addition of the POPD-ZnO composite as a pigment of the WPU coating can effectively prevent further corrosion of the steel sample. The E_{corr} is increased from -0.89 V corresponding to coating free steel surface to -0.62 V after coated PZWC film. Besides the I_{corr} values were found to decrease with coated WPU film (3.63 μA/cm^2), PWC film (1.20 μA/cm^2) and the PZWC film (0.62 μA/cm^2). The decrease in the corrosion current indicates that PZWC and PWC coatings can rely on the reversible redox properties of the polymer materials [32]. In the presence of ZnO nanocomposites, he corrosion resistance of the coating will also increase [33,34]. The results of potentiodynamic curves and EIS indicates that the PoPD and PoPD-ZnO composites inhibit the

Preprints (www.preprints.org) | NOT PEER-REVIEWED | Posted: 12 December 2018 doi:10.20944/preprints201812.0141.v1

anodic reaction by acting as a barrier layer between electrode surface and corrosive environment [24,35].

The protection efficiency (PE%) of coatings was also calculated by the following equation [36]:

$$PE(\%) = \frac{I_{corr} - I'_{corr}}{I_{corr}} \times 100 \quad (2)$$

Where I_{corr} is the corrosion current density of carbon steel and I'_{corr} is the corrosion current density of WPU, PWC and PZWC coatings. Compared to carbon steel, the protection efficiencies for WPU, PWC and PZWC coatings estimated from the above equation are found to be 66.1, 88.8 and 94.2%, respectively.

The corrosion resistances of WPU, PWC and PoPD coated films, evaluated as electrochemical impedance, in 3.5% NaCl solution are presented in (Figure 6b). The solution resistance (R_s), the coating resistance (R_c) and the charge transfer resistance (R_{ct}) were derived from EIS and analyzed by fitting the experimental data to a simple equivalent circuit model in (Figure 6b) and presented in Table 1. The corrosion process of the coating can be further understood by the shape of the Nyquist diagram. The corrosion mechanism controlled by the Nyquist diagram is semi-circular, while the diffusion control is linear. The semicircle in the Nyquist spectrum in (Figure 6b) indicates that the corrosion resistance mechanism of the coating is kinetically controlled. At the same time, a semicircle indicates the occurrence of a corrosion process, which includes the charge transfers resistance caused by metal corrosion and the double layer capacitance of the liquid/metal interface. In the Nyquist diagram, the high frequency region corresponds to the film impedance and the low frequency region represents the charge transfer impedance. The protection efficiencies (PE%) of the charge transfer resistance in Table 1 were calculated by the expression below [29,34]:

$$PE(\%) = \frac{R_{ct} - R^0{}_{ct}}{R_{ct}} \times 100\% \quad (3)$$

Where R_{ct} and R^0_{ct} are the charge transfer resistances of the coated steel and pristine steel, respectively. The value of R_c increased from 229.2 Ω·cm^2 for the WPU film to 259.6 Ω·cm^2 and 914.9 Ω·cm^2 upon the addition of PWC film and PZWC film, respectively. Furthermore, the R_{ct} of WPU, PWC film and PZWC film are 857.2 Ω·cm^2, 928.8 Ω·cm^2 and 1325 Ω·cm^2 resulting in 54.1, 57.6 and 70.3 % protection efficiency, respectively. Among them, the effect of PZWC was most prominent, due to the introduction of ZnO nanoparticles in the polymer matrix resulting in an increase in the surface area of the coating, thereby increasing the charge transfer resistance of the electrode system. One of the special properties of polymers is their ability to interact with the ions liberated during the corrosion reaction of steel in the presence of Cl^- ion [37]. So, their anticorrosion performance increases with the increase of surface area.

Preprints (www.preprints.org) | NOT PEER-REVIEWED | Posted: 12 December 2018 doi:10.20944/preprints201812.0141.v1

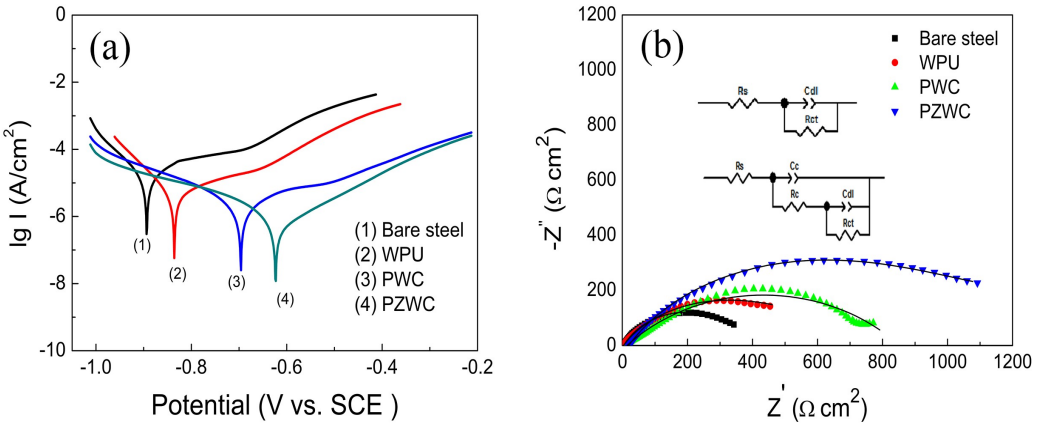

Figure 6. After immersed in 3.5% NaCl solution 168 h, (a) Tafel plots and (b) Nyquist plots of all coatings.

Table 1 Fitting corrosion parameters for all coating surfaces immersed in 3.5% NaCl solution by potentiodynamic curves and EIS.

Coatings	Potentiodynamic curves				EIS				
	E_{corr} (V)	I_{corr} (A/cm^2)	*CR* (mm/year)	*PE* (%)	R_s (Ω·cm^2)	R_c (Ω·cm^2)	R_{ct} (Ω·cm^2)	*PE* (%)	*chi-square*
Bare steel	-0.89	1.07×10^{-5}	1.25×10^{-1}	—	3.4	—	393.5	—	
WPU	-0.84	3.63×10^{-6}	4.23×10^{-2}	66.1	2.83	229.2	857.2	54.1	0.008
PWC	-0.70	1.20×10^{-6}	1.40×10^{-2}	88.8	13.8	259.6	928.8	57.6	0.012
PZWC	-0.62	6.17×10^{-7}	7.20×10^{-3}	94.2	18.8	914.9	1325	70.3	0.003

Both potentiodynamic curves and EIS measurements showed that the PWZC coating provides the best corrosion protection for steel. To further confirm this observation, the appearances and corrosion morphologies of steels surface after immersion to the corrosive medium and removal of the coating were observed and shown in (Figure 7 and Figure 8). Based on the visual appearances and the comparison in (Figure 8), it can be seen that the degree of corrosion of the steel surface after removal of the coatings adapts the following trends: carbon steel > WPU coating > PWC coating > PWZC coating. As shown in (Figure 8a) internal, the metal surface is severely damaged, and the major corrosion pits can be found and some corrosion products were distributed on the steel surface. From (Figure 8b,), (Figure 8c), (Figure 8d), it can be observed that many corrosive white spots can be observed, and the number of spots in the steel surface under the PWC coating is much larger than the steel surface under the WPU coating and the PWZC coating. The area of each corrosion spot is again the largest under the PWC coating. However, after removed the PWZC coating, it can be seen from (Figure 8d) that the steel surface is covered with less amount of corrosion products and corrosion pits compared to the steel surface under the PWC coating. It can be concluded that both electrochemical protection and barrier effects can cause corrosion protection of the composite coating. Electrochemical protection is caused by an increase in the corrosion potential and the formation of a passivation layer on the metal surface.

Preprints (www.preprints.org) | NOT PEER-REVIEWED | Posted: 12 December 2018 doi:10.20944/preprints201812.0141.v1

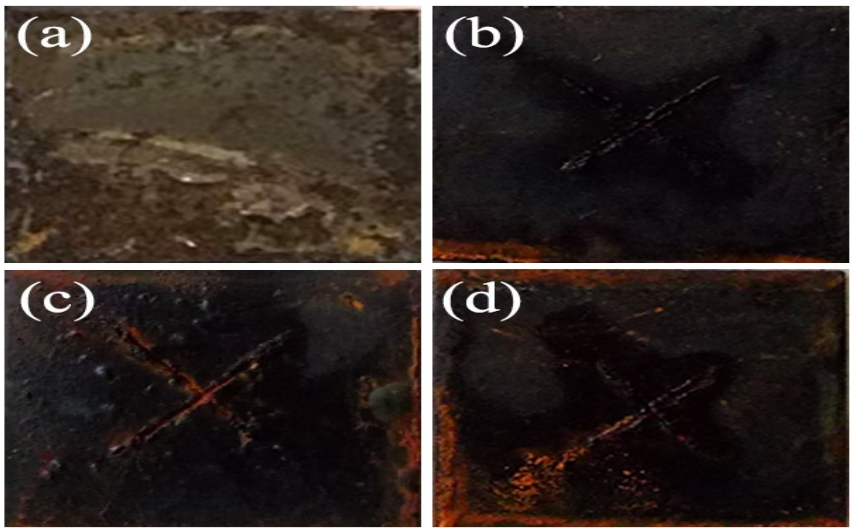

Figure 7. Carbon steel and coatings surface which after soaked in 3.5% NaCl solution for 30 days

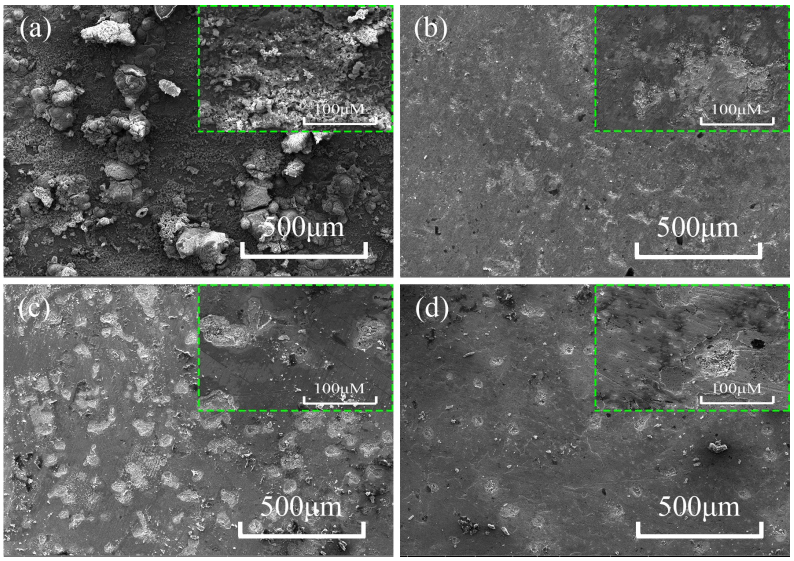

Figure 8. Carbon steel and removed coatings surface which after soaked in 3.5% NaCl solution for 30 days.

3.5 The mechanism of protection

Based on the experiments and their results presented here, the mechanism of corrosion prevention can be described as follows: The conductive polymer can also be reoxidized by reaction with atmospheric or dissolved oxygen. The specific reflection is as follows：

ICP reduction/metal oxidation:

$$(1/n)M + (1/m)ICP^{m+} + (y/n)H_2O \rightarrow (1/n)M(OH)_y^{(n-y)+} + (1/m)ICP^0 + (y/n)H^+$$

ICP oxidation by molecular oxygen:

$$(m/4)O_2 + (m/2)H_2O + ICP^0 \rightarrow ICP^{m+} + mOH^-$$

Therefore, reoxidation of the conducting polymer is necessary for the polymer to continue its

function as an electroactive coating. Further, the reaction of the dopant hydrochloric acid with the carbon steel forms an anti-corrosion film on the carbon steel to produce a metal salt. This insoluble iron-dopant salt will effectively passivate the pinhole as observed. [38].

The addition of an appropriate amount of ZnO nanoparticles to the organic matrix can effectively improve the structure inside the matrix, since these nanoparticles act as obstacles towards the penetration of water molecules and electrolytes. Furthermor, the presence of ZnO increases the tortuosity of those pores, which forces the corrosion agents to travel longer before reaching the substrate surface [39]. Therefore, the corrosion resistance of the coating system is retained for a longer time.

4. Conclusions

The PoPD-ZnO composite was synthesized through an in situ chemical oxidative polymerization method using HCl as the dopant. The structure and morphology of the composite were studied using FT-IR, XRD, and FESEM techniques. The structure studies revealed that morphological studies confirmed that the formation of PoPD-ZnO composites can reduce the size distribution of PoPD. The electrochemical behavior studies revealed that PoPD has a certain degree of reversibility. The corrosion studies of all the coated steel samples immersed in 3.5 wt% NaCl solution by potentiodynamic curves and EIS measurements showed that the PoPD-ZnO composite containing coating exhibits a higher corrosion resistance than that of PoPD, WPU and bare steel. The corrosion rate of PoPD-ZnO coating is two orders of magnitude lower than that of bare steel. The SEM images showed that the corrosion sites on the surface of steel coated with PoPD-ZnO were less than those of coated PoPD, WPU and bare steel, which indicated that the addition of nano-ZnO was beneficial to the barrier performance and corrosion resistance of the PoPD film.

Author Contributions

All authors contributed equally to this work. Jiawei Zhang conceived the idea of the serial PoPD-ZnO material; Chaogang Zhou and Chaojin Zhou directed the experimental work and conducted the measurements. Chaogang Zhou wrote the paper. All authors participated in analyzing the experimental data and discussing the results, as well as preparing the paper.

Conflict of Interests

The author declares that there is no conflict of interests regarding the publication of this paper.

Acknowledgments

We acknowledge financial support from Postdoctoral Daily Funds (No. 3103/14310335), Doctor Startup Foundation Subsidized project of North China University of Science and Technology (No. 28410599).

References

[1] Pour-Ali, S.; Dehghanian, C.; Kosari A. Corrosion protection of the reinforcing steels in chloride-laden concrete environment through epoxy/polyaniline–camphorsulfonate nanocomposite coating. Corros. Sci, 2015, 90, 239-247.

[2] Yamaguchi, I.; Morisaka, R. Synthesis and electrical properties of copolymers of o‐phenylenediamine with aniline, 3,4−ethylenedioxythiophene and 2,3,5,6−tetrafluoroaniline. Polym Int, 2017, 66, 320-326.

[3] Ullah, H.; Shah, A. A.; Ayub K; Bilal, S.; Density functional theory study of

poly(o-phenylenediamine) oligomers. J Phys Chem C, 2013, 117(8), 4069-4078.

[4] Ebrahimi, G.; Neshati, J.; Rezaei, F. An investigation on the effect of H_3PO_4, and HCl -doped polyaniline nanoparticles on corrosion protection of carbon steel by means of scanning kelvin probe. Progress in Organic Coatings, 2017, 105, 1-8.

[5] Samanta, S.; Roy, P.; Kar, P. Structure and properties of conducting poly(o-phenylenediamine) synthesized in different inorganic acid medium. Macromolecular Research, 2016, 24(4), 342-349.

[6] Maryam, B. Y.; Lida, F.; Ali, E.; Maryam, N. Potentiodynamic and electrochemical impedance spectroscopy study of anticorrosive properties of p-type conductive polymer/TiO_2 nanoparticles. Solid State Ionics, 2018, 324, 138-143.

[7] Hosseini, M. G.; Sefidi, P. Y. Electrochemical impedance spectroscopy evaluation on the protective properties of epoxy/DBSA-doped polyaniline-TiO_2 nanocomposite coated mild steel under cathodic polarization. Surface & Coatings Technology, 2017, 331(15), 66-76.

[8] Sambyal, P.; Ruhi, G.; Gairola. S. P.; Dhawan, S. K.; Bisht, B. M. Synthesis & characterization of poly (o-phenitidine)/SiO_2/Epoxy for anti-corrosive coating of mild steel in saline conditions. Materials Research Express, 2018, 5(8), 085307.

[9] Arukalam, I. O.; Meng, M.; Xiao, H.; Ma, Y. Effect of perfluorodecyltrichlorosilane on the surface properties and anti-corrosion behavior of poly(dimethylsiloxane)-ZnO coatings. Applied Surface Science, 2018, 433(1), 1113-1127.

[10] Zhang, F.; Qian H.; Wang, L.; Wang, Z.; Du, C.; Li, X.; Zhang, D. Superhydrophobic carbon nanotubes/epoxy nanocomposite coating by facile one-step spraying. Surface & Coatings Technology, 2018, 341(15), 15-23.

[11] Zheng, H.; Guo, M.; Shao, Y.; Wang, Y.; Liu, B.; Meng, G. Graphene oxide–poly(urea–formaldehyde) composites for corrosion protection of mild steel. Corrosion Science, 2018, 139(15), 1-12.

[12] Tamaddon, F.; Aboee, F.; Nasiri, A. ZnO nanofluid as a structure base catalyst for chemoselective amidation of aliphatic carboxylic acids. Catalysis Communications, 2011, 16(1), 194-197.

[13] Yang, Z.; Zhong, W.; Au, C. T.; Du, X.; Song, H.; Qi, X.; Ye, X.; Xu, M.; Du, Y. Novel Photoluminescence Properties of Magnetic Fe/ZnO Composites: Self-Assembled ZnO Nanospikes on Fe Nanoparticles Fabricated by Hydrothermal Method. Journal of Physical Chemistry C, 2009, 113(51), 21269-21273.

[14] Bairi, V. G.; Bourdo, S. E.; Sacre, N.; Nair, D.; Berry, B. C.; Biris, A. S.; Viswanathan, T. Ammonia gas sensing behavior of tanninsulfonic acid doped polyaniline-TiO_2 composite. Sensors, 2015, 15(10), 26415-26429.

[15] Duran B.; Bereket G.; Turhan M. C.; Virtanen S. Poly(N-methyl aniline) thin films on copper: Synthesis, characterization and corrosion protection. Thin Solid Films, 2011, 519(18), 5868-5874.

[16] Sayyah, S. M.; El-Deeb, M. M.; Kamal, S. M.; Azoon, R. E. Electropolymerization of o−phenylenediamine on Pt−electrode from aqueous acidic solution: Kinetic, mechanism, electrochemical studies and characterization of the polymer obtained. Journal of Applied Polymer Science, 2009, 112(6), 3695-3706.

[17] Gajendran, P.; Saraswathi, R. Electrocatalytic performance of poly(o-phenylenediamine)-Pt–Ru nanocomposite for methanol oxidation. Journal of Solid State Electrochem, 2013, 17, 2741–2747.

[18] Riaz, U.; Jadoun, S.; Kumar, P.; Arish, M.; Rub, A.; Ashraf, S. M. Influence of luminol doping of poly(o-phenylenediamine) on the spectral, morphological, and fluorescent properties: A potential fluorescent marker for early detection and diagnosis of, leishmania

 doi:10.20944/preprints201812.0141.v1

donovani. Acs Appl Mater Interfaces, 2017, 9(38), 33159–33168.

[19] Bilal, S.; Shah, A. U. H. A, Holze, R. Raman spectroelectrochemical studies of copolymers of o -phenylenediamine and o-toluidine. Vibrational Spectroscopy, 2010, 53(2):279-284.

[20] Bilal, S.; Shah, A. U. H. A.; Holze, R. Spectroelectrochemistry of poly(o-phenylenediamine): Polyaniline-like segments in the polymer structure. Electrochimica Acta, 2011, 56(9), 3353-3358.

[21] Gajendran, P.; Vijayanand, S.; Saraswathi, R. Investigation of oxygen reduction at platinum loaded poly(o-phenylenediamine) electrode in acid medium. Journal of Electroanalytical Chemistry, 2007, 601(1-2), 132-138.

[22] D'Elia, L. F.; Ortiz, R. L.; Marquez, O. P.; Marquez, J.; Martinez, Y. Electrochemical Deposition of Poly(o-phenylenediamine) Films on Type 304 Stainless Steel. Journal of The Electrochemical Society, 2001, 148(4), 297-300.

[23] Golgoon, A.; Aliofkhazraei, M.; Toorani, M.; Moradi, M. H.; Rouhaghdam, A. S.; Asgari, M. Corrosion behavior of ZnO-polyester nanocomposite powder coating. Anti-Corrosion Methods and Materials, 2017, 64(4), 380-388.

[24] Ganash A. Anticorrosive properties of poly(o-phenylenediamine)/ZnO nanocomposites coated stainless steel. Hindawi Publishing Corp. 2014, 2014(40), 1-8.

[25] Mobin M, Aslam J, Alam R. Corrosion protection of poly(aniline-co-N-ethylaniline)/ZnO nanocomposite coating on mild steel. Arabian Journal for Science and Engineering, 2017, 42(1), 209-224.

[26] Kannapiran, N.; Muthusamy, A.; Chitra, P.; Anand, S.; Jayaprakash, R. Poly (o-phenylenediamine)/$NiCoFe_2O_4$, Nanocomposites: Synthesis, characterization, magnetic and dielectric properties. Journal of Magnetism & Magnetic Materials, 2017, 423, 208-216.

[27] Wang, J.; Wang, M.; Guan, J.; Wang, C.; W, G. Construction of a non-enzymatic sensor based on the poly(o-phenylenediamine)/Ag-NPs composites for detecting glucose in blood. Materials Science & Engineering C, 2017, 71, 844-851.

[28] Kannapiran, N.; Muthusamy.; A, Renganathan B.; Ganesan, A. R.; Jayaprakash, R. Investigation of magnetic, dielectric and ethanol sensing properties of poly(o -phenylenediamine)/$NiFe_2O_4$, nanocomposites. Journal of Materials Science Materials in Electronics, 2018, 29(4), 3135-3145.

[29] Muthirulan, P.; Rajendran, N. Poly(o-phenylenediamine) coatings on mild steel: Electrosynthesis, characterization and its corrosion protection ability in acid medium. Surface & Coatings Technology. 2012, 206(8-9), 2072-2078.

[30] Samanta, S.; Roy, P.; Kar P. Synthesis of poly(o-phenylenediamine) nanofiber with novel structure and properties. Polym. Adv. Technol. 2017, 28(7), 797-804.

[31] Li, S.; Zhao, C.; Wang, Y.; Li, H.; Li, Y. Synthesis and electrochemical properties of electroactive aniline-dimer-based benzoxazines for advanced corrosion-resistant coatings. Journal of Materials Science, 2018, 53(10), 7344-7356.

[32] Sambyal P.; Ruhi G.; Bhandari H.; Dhawanet S. K. Advanced anti corrosive properties of poly(aniline-co-o-toluidine)/flyash composite coatings. Surface and Coatings Technology, 2015, 272, 129-140.

[33] Najjar, R.; Katourani, S. A.; Hosseini, M. G. Self-healing and corrosion protection performance of organic polysulfide@urea-formaldehyde resin core-shell nanoparticles in epoxy/PANI/ZnO nanocomposite coatings on anodized aluminum alloy. Progress in Organic Coatings, 2018, 124, 110-121.

[34] Mobin, M.; Aslam, J.; Alam, R. Anti-corrosive properties of Poly(aniline-co-2,3-xylidine)/ZnO nanocomposite coating on low-carbon steel. Journal of Adhesion Science & Technology, 2016, 31(7), 749-769.

 doi:10.20944/preprints201812.0141.v1

[35] Mahmoudian, M. R.; Basirun, W. J.; Alias, Y.; Zak, A. K. Electrochemical characteristics of coated steel with poly(N-methyl pyrrole) synthesized in presence of ZnO nanoparticles. Thin Solid Films, 2011, 520(1), 258-265.

[36] Bilal, S.; Farooq, S.; Shah, A. A.; Hoolze, R. Improved solubility, conductivity, thermal stability and corrosion protection properties of poly (o-toluidine) synthesized via chemical polymerization. Synth. Met. 2014, 197, 144-153.

[37] Selvaraj, M.; Palraj, S.; Maruthan, K.; Rajiagopal, G.; Venkatachari, G. Synthesis and characterization of polypyrrole composites for corrosion protection of steel, Journal of Applied Polymer Science, 2010, 116(3), 1524-1537.

[38] Kinlen, P. J.; Menon, V.; Ding, Y. A mechanistic investigation of polyaniline corrosion protection using the scanning reference electrode technique. J. Electrochem. Soc, 1999, 146, 3690-3695.

[39] Ammar, S.; Ramesh, K.; Vengadaesvaran, B.; Ramesh, S.; Arof, A. K. Formulation and characterization of hybrid polymeric/ZnO nanocomposite coatings with remarkable anti-corrosion and hydrophobic characteristics. J. Coat. Technol. Res. 2016, 13(5), 921-930.